HHS Public Access

Author manuscript

Nature. Author manuscript; available in PMC 2020 April 30.

Published in final edited form as:

Nature. 2019 November ; 575(7781): 224–228. doi:10.1038/s41586-019-1708-z.

Human gut bacteria harbor acquired interbacterial defense systems

Benjamin D. Ross[1,†], **Adrian J. Verster**[2,†], **Matthew C. Radey**[1], **Danica T. Schmidtke**[1], **Christopher E. Pope**[3], **Lucas R. Hoffman**[1,3,4], **Adeline M. Hajjar**[5], **S. Brook Peterson**[1], **Elhanan Borenstein**[2,6,7,8,9,*], **Joseph D. Mougous**[1,10,11,*]

[1]Department of Microbiology, University of Washington, Seattle, WA 98195, USA

[2]Department of Genome Sciences, University of Washington, Seattle, WA, 98195, USA

[3]Department of Pediatrics, University of Washington, Seattle, WA, 98195, USA

[4]Seattle Children's Hospital, Seattle, WA, 98105

[5]Department of Comparative Medicine, University of Washington, Seattle, WA 98195, USA

[6]Department of Computer Science and Engineering, University of Washington, Seattle, WA 98195, USA

[7]Blavatnik School of Computer Science, Tel Aviv University, Tel Aviv 6997801, Israel

[8]Sackler Faculty of Medicine, Tel Aviv University, Tel Aviv 6997801, Israel

[9]Santa Fe Institute, Santa Fe, NM 87501, USA

[10]Department of Biochemistry, University of Washington, Seattle, WA, 98195, USA

[11]Howard Hughes Medical Institute, University of Washington, Seattle, WA 98195, USA

Abstract

The human gastrointestinal tract harbors a dense and diverse microbial community, the makeup of which is intimately linked to health. Extrinsic factors such as diet and host immunity are insufficient to explain the constituents of this community, implicating direct interactions between co-resident microbes as an important driver of microbiome composition. The genomes of bacteria derived from the gut microbiome are replete with pathways that mediate contact-dependent interbacterial antagonism[1–3]. Many members of the Gram-negative order Bacteroidales encode the

*Correspondence to: mougous@uw.edu, elbo@uw.edu.

†Equal contribution

Author Contributions: BDR, AJV, AMH, SBP, EB, and JDM designed the study. BDR and DTS performed in vitro growth experiments; AJV, BDR and MCR performed bioinformatic analyses; BDR, CEP, and LRH isolated and sequenced genomes of gut bacteria; BDR, DTS, AMH, and SBP performed gnotobiotic mouse experiments; BDR, AJV, MCR, DTS, AMH, SBP, EB and JDM analyzed data; and BDR, AJV, SBP, EB, and JDM wrote the manuscript.

Competing interests: The authors declare no competing financial interests.

Data and materials availability: *Bacteroides* strains acquired from Johns Hopkins University were obtained under an MTA. All data required to assess the conclusion of this research is available in the main text and supplemental materials, or has been deposited at the Sequence Read Archive under BioProject Accession PRJNA484981.

Code availability: Python and R scripts used in this work are available for download (http://borensteinlab.com/download.html).

type VI secretion system (T6SS), which facilitates the delivery of toxic effector proteins into adjacent cells[4,5]. Here we report the occurrence of acquired interbacterial defense (AID) gene clusters in Bacteroidales residing within the human gut microbiome. These clusters encode arrays of immunity genes that protect against T6SS-mediated intra- and inter-species bacterial antagonism. Moreover, the clusters reside on mobile elements and we demonstrate that their transfer is sufficient to confer toxin resistance *in vitro* and in gnotobiotic mice. Finally, we identify and validate the protective capacity of a recombinase-associated AID subtype (*r*AID-1) present broadly in Bacteroidales genomes. These *r*AID-1 gene clusters have a structure suggestive of active gene acquisition and include predicted immunity factors of toxins deriving from diverse organisms. Our data suggest that neutralization of contact-dependent interbacterial antagonism via AID systems shapes human gut microbiome ecology.

Polymicrobial environments contain a plethora of biotic and abiotic threats to their inhabitants. Bacterial survival in these settings necessitates elaborate defensive mechanisms. Some of these are basal and protect against a wide range of threats, whereas others, for instance CRISPR-Cas, represent adaptations unique to the specific threats encountered by a bacterial lineage[6,7]. In densely colonized habitats such as the mammalian gut, overcoming contact-dependent interbacterial antagonism is likely a major hurdle to survival. The type VI secretion system (T6SS) is a pathway widely utilized by gut bacteria to mediate the delivery of toxic effector proteins to neighboring cells[8–10]. While kin cells are innately resistant to these effectors via cognate immunity proteins, it is unknown whether non-self cells in the gut can escape intoxication. Intriguingly, a number of recent studies have reported that bacteria from a range of environments can encode T6S immunity genes that lack an accompanying cognate effector gene[2,9,11–13]. It has been suggested that these genes play a role in interbacterial defense, but they have yet to be functionally investigated in a physiological context.

To identify potential mechanisms of defense against T6S-delivered interbacterial effectors in the human gut, we mined a large collection of shotgun metagenomic samples (n=553) from multiple studies of the human gut microbiome for sequences homologous to known immunity genes (Supplementary Table 1)[14,15]. We first focused our efforts on *Bacteroides fragilis*, which harbors a well described and diverse repertoire of effector and cognate immunity genes (Supplementary Table 2)[3,8,9]. As expected for genes predicted to reside within the *B. fragilis* genome, sequences mapping to these immunity loci were detected at an abundance similar to that of *B. fragilis* species-specific marker genes in many microbiome samples (Fig. 1a, grey; Supplementary Table 1). However, in a second subset of samples, immunity genes were detected at an abundance significantly higher (>10X) than expected given the abundance of *B. fragilis* (Fig. 1a, blue). Finally, we identified a third subset of samples wherein immunity gene sequences were detected in the absence of *B. fragilis* (Fig. 1a, green). These latter sequences include close homologs of 12 of 14 unique immunity genes (i1-i14) encoded by *B. fragilis* (Extended Data Fig. 1a). In contrast to the pattern observed for immunity genes, we found no samples in which the abundance of corresponding cognate effector genes exceeded that of *B. fragilis* by a significant margin (Fig. 1b, Supplementary Table 1).

The detection of *B. fragilis* immunity gene homologs in samples in which we were unable to detect *B. fragilis* strongly suggests that these elements are encoded by other bacteria in the gut. Indeed, BLAST searches revealed the genomes of several *Bacteroides* spp. that harbor *B. fragilis* T6S immunity gene homologs, including *B. ovatus* (i6, i7, i5, i14), *B. vulgatus* (i8, i13), *B. helcogenes* (i1, i9, i10), and *B. coprocola* (i8, i13). To determine whether these bacteria could also account for the presence of immunity genes in the human gut microbiome, we assembled full-length predicted immunity genes from the metagenomic sequencing reads of individual microbiomes. We limited this assembly to homologs of i6, the most prevalent immunity gene detected in samples lacking *B. fragilis* (Extended Data Fig. 1a). Clustering of the recovered homologs showed that the majority of i6 sequences distribute into three discrete clades that differ by multiple nucleotide substitutions (i6:cI-cIII) (Fig. 2a and Supplementary Table 3). A comparison of these immunity sequences to available bacterial genomes revealed a clade matching cognate immunity genes in *B. fragilis* (i6:cI). Additionally, we found an i6 sequence homologous to i6:cIII in the genome of *B. ovatus*, which we previously found does not contain the cognate T6SS effector gene[8].

To identify the species encoding these sequences in human gut microbiomes, we used a simplified linear model to identify *Bacteroides* spp. whose abundance in microbiome samples best fits that of each immunity sequence clade. We found that i6:cIII is best explained in gut metagenomes by *B. ovatus* (Fig. 2b,c), suggesting that although reference genomes of both *B. fragilis* and *B. ovatus* contain these sequences, it is most often harbored by the latter in natural populations. We could not confidently define a single species harboring i6:cII by this method (Fig. 2d,e); therefore, we employed the same analysis pipeline to an infant microbiome dataset for which matching stool samples were available[16] (Extended Data Fig. 1b and Supplementary Table 4). Whole genome sequencing of isolates identified *B. xylanisolvens* as a bacterium harboring i6:cII in these samples. Notably, this species best fit the abundance of i6:cII genes in the large adult metagenomic datasets, albeit by a narrow margin (Fig. 2d). Based on these observations, we hypothesized that orphan immunity genes – encoded by *B. fragilis* and other species of *Bacteroides* – serve an adaptive role in the gut by providing defense during intra- and inter-species antagonism.

To gain insight into the function of orphan immunity genes, we examined their genomic context in available reference genomes and assembled sequence scaffolds from metagenomic data. We found that homologs of *B. fragilis* T6S immunity genes i6 and i7 are located together within discrete gene clusters, which we termed AID-1 (acquired interbacterial defense 1) systems, in several *Bacteroides* strains and in microbiome samples (Fig. 2f). Within AID-1, we identified distant homologs and pseudogenized remnants of additional *B. fragilis* immunity genes, including i4, i5, i11, and i14 (Fig. 2f and Supplementary Table 5). These findings prompted us to search for more distant homologs of *B. fragilis* T6S immunity genes. This revealed gene clusters containing orphan homologs of i1, i3, i8, i9, i10, and i13 in diverse *Bacteroides* genomes and we also identified distant homologs of these genes in a metagenomic gene catalog (Extended Data Fig. 2a,b). In *B. xylanisolvens*, we found that genes belonging to i6:cII are located in a unique, but analogous context adjacent to a homolog of i5 on an apparent transposable element (Fig. 2g)[17]. We designated this sequence AID-2.

We next defined the phenotypic implications of orphan immunity genes of *Bacteroides* spp. during interbacterial competition. *B. fragilis* 9343 encodes the cognate effectors for i6 and i7, and prior data demonstrate that the corresponding toxins antagonize assorted *Bacteroides* spp. *in vitro* and in gnotobiotic mice[9]. We thus employed this strain in growth competition assays against *Bacteroides* spp. bearing orphan immunity genes, derivative strains containing deletions of these genes, or genetically complemented strains. These experiments showed that in both *B. ovatus* and *B. fragilis*, AID-1 system genes grant immunity against corresponding T6S effectors (Fig. 3a, Extended Data Fig. 3a,b). The i6 and i7 genes of *B. ovatus* did not influence the outcome of its competition with *B. fragilis* 638R, which possesses an orthogonal effector repertoire (Extended Data Fig. 3c). Finally, we also found that an i6:cII gene from a *B. xylanisolvens* AID-2 system affords this bacterium protection against e6 of *B. fragilis* 9343 (Fig. 3b). In total, these data show that the orphan immunity genes of multiple *Bacteroides* spp. – localized to AID systems – can confer protection against effectors delivered by the T6SS of *B. fragilis*.

B. fragilis is typically found as a clonal population in the human gut microbiome, and recent studies suggest that this is in part due to active strain exclusion via the T6SS[8,18]. However, in gnotobiotic mouse colonization experiments, certain *B. fragilis* strain pairs inexplicably co-exist[10]. We noted that one such pair corresponds to *B. fragilis* 9343 and *B. fragilis* 638R, the latter of which contains an AID-1 system harboring homologs of i6 and i7. To determine whether our *in vitro* results with these strains extend to a more physiological setting, we measured the fitness contribution of the orphan immunity genes encoded by *B. fragilis* 638R following pre-colonization of germ-free mice with *B. fragilis* 9343 (Fig. 3c, Extended Data Fig. 3d, e). Our results indicated that the cumulative protection afforded by orphan i6 and i7 genes underlies the capacity of *B. fragilis* 638R to persist during T6S-mediated antagonism *in vivo*.

Interestingly, we found that AID-1 resides on a predicted mobile integrative and conjugative element (ICE), potentially providing an explanation for its distribution (Fig. 3d)[19]. To test whether this element can be transferred between strains, we performed mobilization studies using *B. fragilis* 638R as a donor and *B. fragilis* 43859 as a recipient. An antibiotic resistance marker was inserted within AID-1 to facilitate the detection of its transfer. With this tool, we readily detected AID-1 transfer (Fig. 3e). This occurred at a frequency of approximately 5×10^{-6}, in line with previous quantification of ICE mobility in *Bacteroides* spp.[20]. Next, we asked whether the transfer of AID-1 to *B. fragilis* 43859 is sufficient to confer resistance to T6S-mediated antagonism. *In vitro* growth competition assays against *B. fragilis* 9343 showed that AID-1 effectively neutralizes intoxication by e6 and e7 (Fig. 3f). The receipt of AID-1 also granted significant protection to *B. fragilis* 43859 against T6-mediated killing in germ-free mice pre-colonized with *B. fragilis* 9343 (Fig. 3g). Together, these findings indicate that the transfer of a mobile orphan immunity island to a naïve *Bacteroides* strain is sufficient to provide defense against T6S effectors.

Deciphering the contribution of individual gene products, or even whole pathways, to bacterial fitness in complex microbial communities is challenging. We reasoned that the ability to identify orphan immunity genes in human gut metagenomes, coupled with our capacity to infer their organismal source, provided an opportunity to measure the impact of

these defensive factors on competitiveness in the gut. To this end, we compared the abundance of *B. ovatus* strains with and without i6 and i7 orphan immunity genes in human gut metagenome samples. Interestingly, we found that the average abundance of *B. ovatus* strains with orphan immunity genes significantly exceeds that of those without (Extended Data Fig. 3g). One interpretation of this finding is that the acquisition of i6 and i7 allows *B. ovatus* to increase its niche; however, there are several potential caveats inherent to these correlative data that cannot be ruled out. For instance, *B. ovatus* strains containing i6 and i7 might be related and enriched for other fitness determinants that account for their abundance.

Given the benefit of orphan immunity genes against *B. fragilis* effectors, we hypothesized that this mechanism of inhibiting interbacterial antagonism should extend to effectors produced by other species. We previously reported evidence that *B. fragilis* is antagonized by other *Bacteroides* spp. in the human gut microbiome[8]. In addition to the T6SS present exclusively in *B. fragilis*, this species and other *Bacteroides* spp. can possess other T6SSs, referred to as GA1 (genetic architecture 1) and GA2, with a distinct and non-overlapping repertoire of effector and immunity genes[3]. The effectors of these systems exhibit hallmarks of antibacterial toxins and we demonstrated their capacity to mediate interbacterial antagonism (Fig 4, Extended Data Fig. 4)[2,8]. Therefore, we searched *B. fragilis* genomes for sequences homologous to the immunity genes corresponding to these systems. In 29 of the 122 available *B. fragilis* genomes, we identified apparent orphan homologs of these immunity genes grouped within gene clusters (Fig. 4a). While analogous to the AID-1 and −2 systems, these clusters have several unique characteristics including skewed GC content, conservation of a gene encoding a predicted XerD-family tyrosine recombinase, and repetitive intergenic sequences (Extended Data Fig. 5a–c)[21]. These often-large gene clusters, hereafter referred to as recombinase-associated AID (*r*AID-1) systems, can exceed 16 kb and contain up to 31 genes with varying degrees of homology to T6S immunity genes and predicted immunity genes associated with other interbacterial antagonism pathways (Fig. 4a, Extended Data Fig. 5d, e, Supplementary Table 6)[2]. Using the shared characteristics of *B. fragilis r*AID-1 systems, we searched for related gene clusters across sequenced Bacteroidales genomes. We found that over half of sequenced bacteria belonging to this order possess a *r*AID-1 system (226 of 423) (Fig. 4b, Supplementary Tables 6,7). In sum, these gene clusters contain 579 unique genes, encompassing homologs of 25 Bacteroidales T6S immunity genes.

The prevalence of *r*AID-1 genes in Bacteroidales genomes suggested that these elements may be common in the human gut microbiome. To investigate this, we searched metagenomic data for sequences mapping to Bacteroidales T6S orphan immunity genes found within *r*AID-1 systems. Remarkably, we found one or more *r*AID-1 immunity genes in 551 of 553 samples using a 97% sequence identity threshold to map reads (Supplementary Table 8). These *r*AID-1 immunity genes diverge significantly from corresponding cognate immunity genes (corresponding to 32–91% amino acid identity), suggesting that the latter are an unlikely source of significant false positives in this analysis. We also searched the same samples for *r*AID-1-associated recombinase sequences. Although recombinase genes are widely distributed across bacteria, close homologs (>50% amino acid identity) of those found associated with *r*AID-1 systems are restricted to this context and

only found in Bacteroidales genomes. Consistent with this, we found the abundance of *r*AID-1 recombinase genes correlates strongly with the genus *Bacteroides* (Extended Data Fig. 5f).

Orphan immunity genes encoded within *r*AID-1 clusters diverge more significantly from cognate immunity than do those within AID systems. Thus, we sought to experimentally validate the capacity of *r*AID-1 immunity genes to protect bacteria from intoxication. Since most bacteria harboring *r*AID-1 systems have limited genetic tools, we employed *E. coli* to identify three Bacteroidales T6S effector genes that intoxicate cells in a manner that is neutralized by cognate immunity. In each case, we found that co-expression of these effector genes with corresponding *r*AID-1-associated orphan immunity genes, but not mismatched orphan immunity genes, restored *E. coli* growth (Fig. 4c). Both genes from one effector–orphan immunity pair we validated derive from genetically tractable strains: *B. fragilis* YCH46 (effector, 2850) and *B. fragilis* 9343 (orphan immunity, 08050). *In vitro* growth competition experiments with these strains, and mutant and genetically complemented derivatives, showed that an endogenous *r*AID-1 orphan immunity gene of *B. fragilis* 9343 can neutralize a T6S-delivered toxin (Fig. 4d).

The orphan immunity systems we defined consist of many genes and their expression could incur a substantial metabolic burden. As a first step toward understanding the regulation of AID systems, we performed quantitative RT-PCR to compare the expression of the systems in the presence and absence of a competitor strain. These studies provided evidence that transcription of both systems is induced by co-cultivation with a competitor strain (Extended Data Fig. 5g). We also examined metatranscriptomic data for evidence of AID expression[22]. Owing to a paucity of such data available for samples definitively containing AID-1 and AID-2, we could not systematically quantify expression of these systems. However, using conservative criteria for defining *r*AID-1-associated genes in metatranscriptomic data, we found evidence of the expression of this system in every sample derived from a large study (n=156) (Supplementary Table 9). In some samples, such as those with high levels of *Bacteroides*, *r*AID-1 genes accounted for nearly 1/10,000 of all metatranscriptomic reads. Taken together with our functional characterization of AID systems, these findings suggest that acquisition and maintenance of consolidated orphan immunity determinants is a common mechanism by which Bacteroidales defend against interbacterial antagonism in the human gut microbiome.

Mounting evidence suggests that competitive interactions between bacteria predominate in many environments[23]. This evolutionary pressure has undoubtedly led to the wide dissemination of idiosyncratically orphaned immunity genes predicted to provide resistance to diverse antagonistic pathways[2,11,24,25]. Modeling studies predict that interbacterial antagonism is a critical contributor to the maintenance of a stable gut community[26]. Our findings reveal that a corollary of the pervasiveness of antagonistic mechanisms is strong selective pressure for genes that can provide protection against attack, establishing a molecular arms race that has led to diversification and expansion of T6S effectors. Deciphering the linkage between orphan immunity genes and the bacteria harboring the cognate effectors has the promise of providing a window into the physical connectivity of bacteria in the gut microbiome.

It is now appreciated that phage defense mechanisms, including the adaptive system, CRISPR, are critical for bacteria to cope with the omnipresent threat and deleterious outcome of phage infection[7]. However, the ubiquity of interbacterial antagonistic systems suggests that in most habitats, bacteria are equally, or perhaps more likely to be subject to attack and potential cell death via the action of other bacteria[2]. Our characterization of AID systems encoded by prevalent members of the human gut microbiota appears to reconcile these observations and demonstrate that the neutralization of contact-dependent interbacterial antagonism can be a critical mechanism for survival in polymicrobial environments. Additionally, it suggests that analogous to the immune system of vertebrates, that of bacteria includes arms specialized in viral or bacterial defense.

Material and Methods

Microbiome Data

Metagenomic data from healthy adults were obtained from a number of large-scale sequencing projects. We specifically obtained 147 samples from the Human Microbiome Project 1.0, 100 samples from HMP 1.2, and 99 and 207 samples from two different MetaHIT datasets[14,15,29,30]. We further obtained paired metagenomic-metatranscriptomic data from a study of 156 individuals[22]. Finally, we obtained a database of genes identified from 1267 assembled metagenomes as part of the Integrated Gene Catalogue (IGC)[27].

Analysis of gene and species abundances in microbiome samples

We previously compiled a list of T6SS immunity and effector genes[8]. We additionally compiled a list of species-specific marker genes for all *Bacteroides* species obtained from MetaPhlAn 2.0[31]. In order to determine the abundance of a given immunity, effector, or marker gene in each metagenomic sample, single end metagenomic reads were aligned to gene sequences using bowtie2, allowing for one mismatch in the seed[32]. We counted the number of reads that aligned to each such gene with at least 80% nucleotide identity (to encompass divergent orphan immunity gene sequences) and minimum mapping quality of 20. The abundance of a gene was calculated as the number of reads aligned to this gene, normalized by the gene length and by the library size. For each species, the average gene level abundance of all species-specific marker genes was used to assess the species abundance. For the total *Bacteroides* abundance, we used the sum of all species-specific marker genes in the genus. Samples were only included in an analysis if they had at least 10 reads mapping to the type 6 genes in question (effectors, immunity or recombinases). Based on the abundance of GA3 immunity genes and *B. fragilis* we split samples into those where *B. fragilis* was not detectable, those where the immunity gene had >10X the *B. fragilis* marker gene abundance, and those where such discrepancy between the abundance of immunity genes and that of *B. fragilis* was not observed. Metatranscriptomics data was processed similarly to metagenomics data, except that abundance values were converted to an RPKM for familiarly with canonical RNA-Seq analysis.

Orphan immunity phylogenetic analysis

Filtered reads derived from human shotgun microbiome datasets were aligned using bowtie2 as described above and subsequently converted to a pileup using samtools with parameters --

excl-flags UNMAP,QCFAIL,DUP -A -q0 -C0 -B[32,33]. A sequence corresponding to the most abundant version of the immunity gene in the sample was reconstructed from that pileup as follows. First, 50 bases from the start and end were trimmed due to a propensity for low coverage. Second, at all sites with at least 10X coverage the base was set to the major allele. Sites with <10X coverage were assigned an ambiguous base. Finally, we only kept the reconstructed sequence in metagenomic samples where at least 90% of the sequence had >10X coverage. The number of SNPs between all immunity sequences, both from metagenomic samples and from *Bacteroides* genomes, was calculated and used to populate a distance matrix. Since obtained distances were small (e.g., a single base difference), we used hierarchical clustering (with complete linkage), rather than standard phylogenetic reconstruction methods, to visualize the relatedness between different sequences. Sequence clades defined by hierarchical clustering are denoted (cI-III), as discussed in the text.

Assigning orphan immunity sequences to bacterial species

We aimed to identify the species most likely to encode the immunity gene in each cluster of identical sequences reconstructed from metagenomes. Only clusters with at least 3 sequences were used, to ensure statistical confidence. The abundance of each species was assessed based on species-specific marker genes as described above. We specifically employed a simple linear model that assumed that only a single species encodes the immunity gene. We further assumed a one to one relationship between species marker gene abundance and orphan immunity gene abundance, and accordingly fixed the intercept at zero and allowed a single species with a slope of one. The fit of the model for each species was calculated as the mean square error over all samples. The most likely species to encode the immunity gene was determined by the minimum mean squared error.

Assembly of orphan immunity sequences from metagenomes

Paired-end metagenomic sequencing data was assembled using SoapDeNovo2 with a kmer length of 63 and an average insert size of 200[34]. BLAST was used to identify the contig that contained the orphan immunity gene, and GeneMarkS was used to predict protein coding genes[35].

Bacterial culture conditions

Anaerobic culturing procedures were performed either in an anaerobic chamber (Coy Laboratory Products) filled with 70% N_2, 20% CO_2 and 10% H_2, or in Becton Dickson BBL EZ GasPak chambers. *E. coli* EC100D λ pir and S17–1 λ pir strains were grown aerobically at 37° C on lysogeny broth agar. Unless otherwise noted, *Bacteroides* strains were cultured under anaerobic conditions on brain heart infusion agar (BHI; Becton Dickinson) supplemented with 50 μg mL^{-1} hemin and 10% sodium bicarbonate[36]. Antibiotics and chemicals were added to media as needed at the following concentrations: trimethoprim 50 μg mL^{-1}, carbenicillin 150 μg mL^{-1}, gentamicin 15 μg mL^{-1} (*E. coli*), gentamicin 60 μg mL^{-1} (*Bacteroides*), erythromycin 12.5 μg mL^{-1}, tetracycline 6 μg mL^{-1}, chloramphenicol 12 μg mL^{-1}, floxuridine (FUdR) 200 μg mL^{-1}.

Genetic techniques

Standard molecular procedures were employed for creation, maintenance and *E. coli* transformation of plasmids. All primers used in this study were synthesized by Integrated DNA Technologies (IDT). Phusion polymerase, restriction enzymes, T4 DNA ligase, and Gibson Assembly Reagent were obtained from New England Biolabs (NEB). A comprehensive list of primers, plasmids, and strains are provided (Supplementary Table 10). Deletion of the gene encoding thymidine kinase in *B. fragilis*, *B. ovatus*, and *B. xylanisolvens* strains was performed by cloning respective genomic flanking regions into the vector pKNOCK as previously described[37]. Briefly, pKNOCK-*tdk* plasmids were mobilized into *Bacteroides* strains via overnight aerobic mating with *E. coli*. Integrants were isolated by plating on selective media, were passaged once without antibiotics to allow for plasmid recombination, and plated for counter selection on FUdR. Recovered single colonies were patched onto selective media to ensure loss of pKNOCK, and disruption of *tdk* confirmed by PCR. Subsequent deletion of orphan immunity genes was performed in Δ*tdk* strains via a similar counter selection strategy, except employing the suicide plasmid pExchange in place of pKNOCK[9]. Genomic deletions were confirmed by PCR. Gene complementation was performed by cloning genes into pNBU2-erm_us1311 for constitutive expression[38].

Isolation of *Bacteroides* strains from fecal samples

Fecal samples from healthy infants used for strain isolation were collected as part of a prior study approved by the Seattle Children's Hospital Institutional Review Board[16,39]. Frozen stool samples stored at −80° C were manually homogenized, serially diluted in tryptone yeast glucose (TYG) broth, and plated under anaerobic conditions on *Bacteroides* bile esculin (BBE) agar plates (Oxyrase, Inc). Single colonies which exhibited esculin hydrolysis as indicated by the production of black pigment on BBE agar were sub-cultured in TYG broth with the addition of 60ug/mL gentamicin until stationary phase and then were frozen at −80° C following the addition of sterile glycerol to 20% final concentration. Single colonies isolated from these stocks were subsequently screened by PCR with primers targeting the orphan i6 gene as assembled from metagenomic short read sequence data[16].

Genome sequencing

Genomic DNA used for Illumina sequencing was prepared by harvesting *Bacteroides* strains grown overnight on BHIS blood agar plates. Cells resuspended from plates were washed in phosphate buffered saline before DNA extraction with the Qiagen DNeasy Blood and Tissue Kit. Sequencing was performed on an Illumina MiSeq using the V3 Reagent kit at the Northwest Genomics Center sequencing facility at the University of Washington. AID clusters often appear in highly repetitive genomic contexts (e.g. mobile elements) and are often split into multiple scaffolds in reference genomes. To compensate for this, we additionally performed long read sequencing via PacBio on a subset of genomes. To this end, high-molecular weight DNA was extracted using the Qiagen Genomic-tip Kit and sequenced by SNPsaurus (Eugene, OR) using a PacBio Sequel. Hybrid long read-short read assemblies were conducted using Unicycler[40]. Species identification was performed by blast searches with species-specific marker genes[31]. Whole genome sequencing data generated in

the course of this study has been deposited at the Sequence Read Archive under BioProject Accession PRJNA484981.

Interbacterial competition assays

Bacteroidales strains were grown on BHIS blood agar plates overnight at 37° C. Bacteria were resuspended from plates in BHIS broth and the optical density of each strain was adjusted to a 10:1 *B. fragilis* NCTC 9343 to competitor ratio (OD_{600} 6.0 to 0.6) for competitions involving *B. xylanisolvens* and *B. ovatus*, or 1:1 ratio for competitions involving *B. fragilis* 638R (OD_{600} 6.0). Equal volumes of each strain at the adjusted OD were mixed and 5ul of bacterial mixtures were spotted onto pre-dried BHIS blood agar plates, in triplicate spots. Competitions were allowed to proceed for 20–24 hours at 37° C under anaerobic conditions before spots were harvested into BHIS broth. Competition outcomes were quantified in one of two ways: 1) by serial dilution for enumeration of colony forming units after plating on BHIS selective plates containing either erythromycin or tetracycline, or 2) purification of total genomic DNA using the Qiagen DNeasy Blood and Tissue Kit and subsequent quantification by qPCR using strain-specific primers (see Supplementary Table 10). For antibiotic selection, *B. fragilis* 9343 was marked with erythromycin resistance by integration of pNBU2-erm at the att1 site[38]. Other strains were either naturally tetracycline resistant, or were marked by integration of pNBU2-tet-BCO1. Strains with insertions of pNBU2 were selected for matching integration sites by PCR with primers flanking att loci[41]. Interbacterial competitions between strains of *B. fragilis* occasionally exhibited T6SS-independent phenotypes that were dependent on the initial starting ratio of the strains used[42].

Interbacterial mobile element transfer assays

Allelic exchange was used to engineer a high-expression chloramphenicol resistance cassette onto the AID-1 system of *B. fragilis* 638R, replacing BF638R_2056–2058[43]. Chloramphenicol-resistant *B. fragilis* 638R cells were mixed on BHIS blood agar plates with erythromycin-resistant *B. fragilis* ATCC 43859 cells at a 1:1 ratio (OD_{600} 6.0). Following overnight co-culture, bacterial mixtures were harvested and plated on BHIS plates containing either erythromycin alone (to quantify c.f.u. of total ATCC cells), or erythromycin and chloramphenicol (to quantify c.f.u of AID-1 recipient ATCC cells). Doubly-resistant colonies were screened individually by PCR to confirm strain identity, the presence of the AID-1 system, and the genomic integration site at a tRNA-Lys gene (see Supplementary Table 10 for primers used).

Gnotobiotic animal studies

Germ-free 6–12 week-old female Swiss Webster mice from multiple litters were randomized, housed simultaneously in pairs in single Techniplast cages with a 12-hour light/dark cycle, and fed a standard lab diet (Laboratory Autoclavable Rodent Diet 5010, LabDiet), in accordance with guidelines approved by the University of Washington Institutional Animal Care and Use Committee. Blinding was not performed, and no statistical methods were used to determine sample size. Reasonable numbers of animals were used considering limitations of housing and maintenance under gnotobiotic conditions.. *Bacteroides fragilis* strains were introduced into mice via oral gavage of 10^8

colony forming units (c.f.u.) suspended in 0.2mL of sterile 1X phosphate buffered saline with 20% glycerol. Challenge with *B. fragilis* 638R or *B. fragilis* ATCC strains occurred 7 days following pre-colonization with *B. fragilis* 9343 strains. Colonization levels by each strain in each mouse were tracked by collection of fecal pellets over a period of 4 weeks, plating on selective BHIS agar plates (*B. fragilis* 9343 on BHIS plus erythromycin; *B. fragilis* 638R and ATCC on BHIS plus tetracycline), and subsequent absolute quantification of c.f.u. by normalization of each sample to the initial pellet weight. Differences in the strain ratio of c.f.u between groups at each timepoint was assessed using Mann Whitney U tests. Non-parametric tests were used following Shapiro-Wilk analysis for normality of data at each time point. Mice were confirmed to be sterile prior to colonization by qPCR with primers targeting the 16S rRNA gene and free of non-*Bacteroides* contamination by plating fecal pellets on non-selective LB and BHIS plates incubated under either anaerobic and aerobic conditions[44].

Bioinformatic analysis of *r*AID-1 clusters

The amino acid sequence of the *B. fragilis* NCTC 9343 polyimmunity-associated XerD-like tyrosine recombinase (BF9343_RS08045) was used as a query against a custom database of 423 *Bacteroidales* genomes downloaded from GenBank. *r*AID clusters in *Bacteroidales* genomes were identified based upon the following criteria: i) presence of a 5' XerD-like tyrosine recombinase gene encoding a protein with amino acid identity exceeding 44% (corresponding to an e-value of 10^{-100}), ii) 2 or more co-directionally oriented downstream genes which possessed iii) a GC content of 41% or lower. The end of the gene cluster was defined as the stop codon of the last co-directionally oriented gene in the cluster with similar GC content. To identify homologs of genes within *r*AID clusters, open reading frames within the clusters were translated and used as tblastn queries against the NCBI non-redundant nucleotide database. Top hits from these searches were often genes in other *r*AID clusters; therefore, these hits were discarded. The top non-*r*AID hit from tblastn searches with an e-value threshold of 10^{-30} was selected as the closest homolog. *r*AID cluster genes were assigned to interbacterial immunity gene families via hmm scans with profiles from Zhang *et al.*[2] with an e-value cutoff of 10^{-3}. *r*AID cluster genes were additionally compared via tblastn with forty-six Bacteroidales T6SS immunity genes from subtypes 1–3[3,8] with an e-value cutoff of 10^{-10}. Percent amino acid identity with homologs was assessed if sequences could be aligned across ≥80% of their length. Motif enrichment analysis was performed on non-coding sequences within a subset of *r*AID-1 clusters (14 sequences immediately 3' of the recombinase stop codon, and 86 intergenic sequences between *r*AID-1 ORFs), using MEME Suite 5.0.2 and default settings[28].

Heterologous expression of *Bacteroides* toxin and immunity genes

To assess the ability of cognate immunity or orphan immunity to neutralize the toxicity of a *Bacteroidales* T6SS effector, genes were cloned into *E. coli* expression vectors pScrhab2-V (effectors) and pPSV39-CV (immunity). Immunity genes were fused with the *P. aeruginosa* ribosome binding site from *hcp1* during the cloning process[45]. All cloning steps for effector genes involved growth of *E. coli* on media containing 0.1% glucose to ensure repression of expression. *E. coli* DH5a cells were co-transformed with pSchraB2 and pPSV39 plasmids bearing genes of interest. Overnight cultures were then grown from single co-transformed

colonies to stationary phase in LB broth containing 50ug/mL trimethoprim, 15ug/mL gentamycin, and glucose. Cells were harvested from these cultures and washed to remove glucose before back-dilution to an OD_{600} of 0.05 into LB broth containing 50ug/mL trimethoprim, 15ug/mL gentamycin, 0.05% rhamnose, and 1mM isopropyl β-D-1-thiogalatopyranoside[45,46]. Cultures were then grown for 8 hours shaking at 37°C before plating to allow quantification of c.f.u. Experiments were performed with technical triplicates for each of at least two biological replicates.

Gene expression analysis of AID-1 and *r*AID-1 systems of *B. ovatus* 3725

To assess the level of expression of genes in the AID-1 and *r*AID-1 systems of *B. ovatus* 3725, bacterial cells were first grown overnight on BHIS blood agar plates containing gentamycin. Cells were then resuspended in BHIS to an OD_{600} of 3.0 for *B. ovatus* monocultures, or to an OD_{600} of 0.3 for mixed co-culture experiments with *B. fragilis* 9343 at 10-fold excess (OD_{600} of 3.0). 5uL volumes of bacterial mixtures were then spotted on BHIS blood agar plates. Plates were incubated at 37°C for 2 hours under anaerobic culture conditions before cells were harvested directly in Buffer RLT plus (twenty 5uL spots per condition per replicate, Qiagen RNeasy Micro Kit). Two separate rounds of DNase treatment were performed (Qiagen RNase-free DNase, Thermo Fisher Scientific Turbo DNase-free kit). RNA samples were confirmed to be free of genomic DNA by PCR with primers targeting the Bacteroides 16S rRNA gene. cDNA was generated using the High Capacity cDNA Reverse Transcription Kit (Applied Biosciences). Following synthesis, cDNA was diluted 1:10. Quantitative PCR (primers listed in Supplementary Table 10) was performed using SSO Universal SYBR Green Supermix (Bio-Rad) on a CFX96 machine (Bio-Rad). Genomic DNA was used to generated standard curves[47]. Differences in gene expression between samples was performed by normalization to the expression level of *B. ovatus* 3725 *gyrB*. Primers targeting *gyrB* were designed to target regions of the genes that are highly polymorphic between *B. fragilis* and *B. ovatus*, and species-specificity for *B. ovatus* was confirmed by PCR using *B. fragilis* genomic DNA[48].

Extended Data

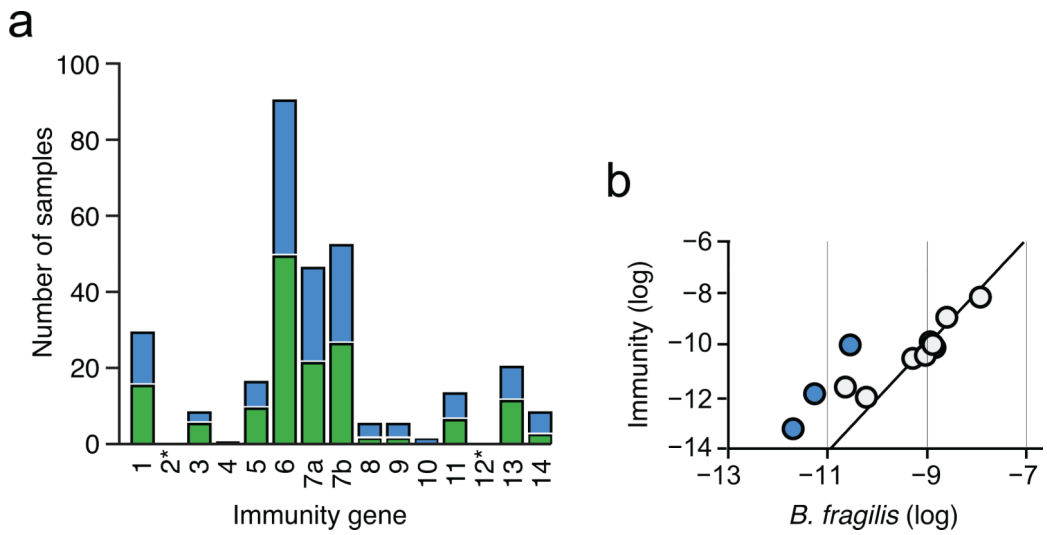

Extended Data Fig. 1 |. Prevalence of *B. fragilis*-specific orphan immunity genes in adult and infant microbiomes.

a, Number of adult human gut microbiome samples in which the indicated immunity genes (1–14, GA3_i1–14 from ref[8]) can be detected at an 80% nucleotide identity threshold and an abundance >10-fold that of *B. fragilis* marker genes. Bars colored corresponding to Fig. 1a and asterisks indicate immunity genes without orphan representation. **b**, Abundance comparison of *B. fragilis*-specific T6SS immunity genes with *B. fragilis* species-specific marker genes in infant microbiome samples (Supplementary Table 4)[16]. Abundances are calculated as in Fig. 1a. Samples in which immunity gene abundance exceeds that of *Bacteroides* by over 10-fold (blue) are highlighted.

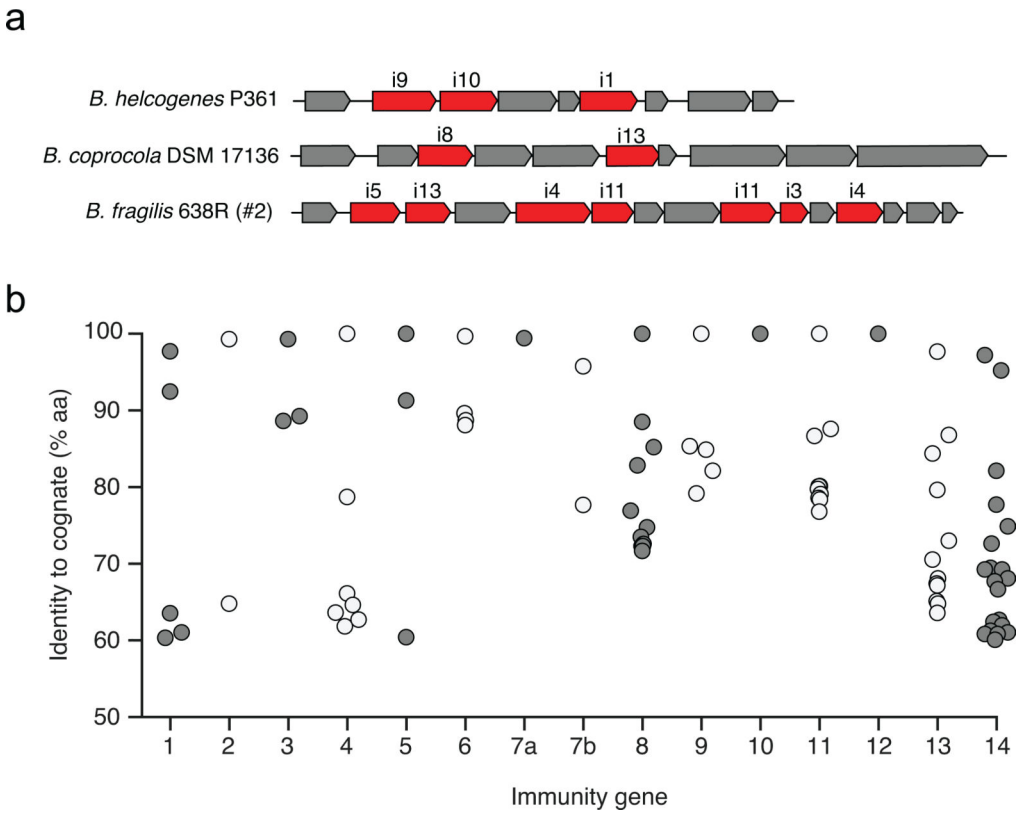

Extended Data Fig. 2 |. Diversity and genomic context of orphan immunity genes in human gut microbiomes and diverse *Bacteroides* species.

a, Representative AID-1 gene clusters containing homologs of the indicated *B. fragilis* T6S immunity genes from the indicated reference genomes. **b,** Data points indicate the amino acid identity of unique genes homologous to indicated *B. fragilis*-specific T6SS cognate immunity genes identified through BLAST analysis of the Integrated Gene Catalog (IGC) (n=88 genes, maximum E-value, 10^{-40}; minimum percent identity, 60%)[27].

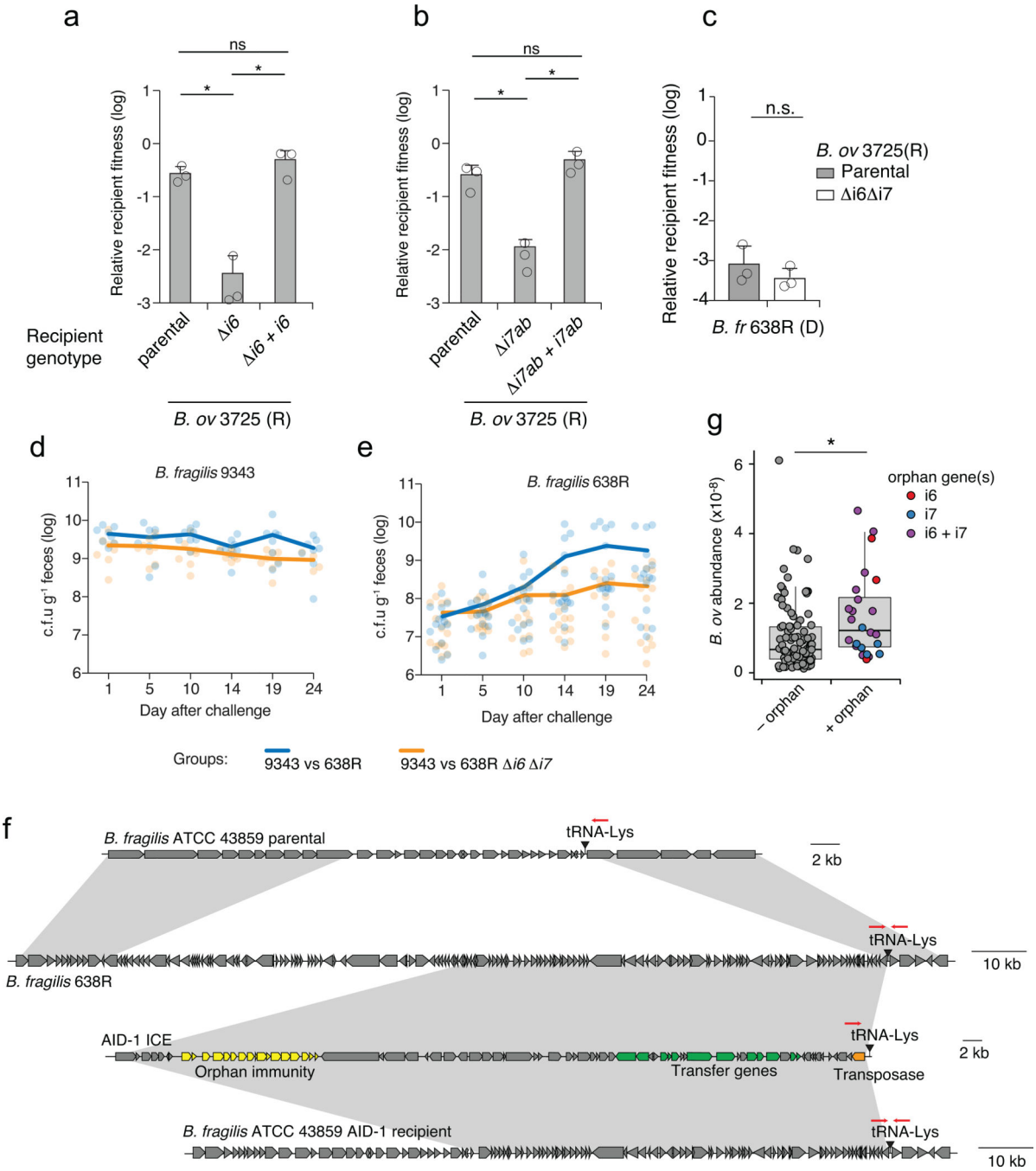

Extended Data Fig. 3 |. Orphan immunity genes specifically enhance the fitness of *Bacteroides* strains *in vitro* and *in vivo*.

a, b, T6SS-dependent competitiveness of parental strains of *B. ovatus* 3725 and the indicated mutant and complemented derivatives during *in vitro* growth competition experiments with *B. fragilis* 9343. Relative recipient fitness was determined by calculating the ratio of final to initial colony forming units and normalizing to the corresponding experiment with *B. fragilis* 9343 lacking *tssC* (T6S-inactive). Data represent mean ± s.d. of n=3 independent biological replicates, unpaired two-tailed t-test, $*P < 0.01$. **c,** T6SS-dependent

competitiveness of a parental strain of *B. ovatus* 3725 or a strain bearing in-frame deletions of indicated orphan immunity genes, during *in vitro* growth competition experiments with an orthogonal effector-bearing *B. fragilis* 638R parental strain or a derivative strain lacking *tssC* (T6-inactive). Relative recipient fitness and statistics were calculated as in **a**, **b**, n=3 independent biological replicates. **d, e,** Recovery of *B. fragilis* 9343 **d,** or 638R and the indicated orphan immunity mutant derivative **e,** from pairwise competitions of the strains in germ-free mice. Lines indicate the mean at each time point, (n=8 mice per group for each of two independent experiments). Alternating time points of these data are included in ratio form in Fig. 3c. **f,** Schematic depicting genomic loci for the *B. fragilis* ATCC 43859 parental strain, the *B. fragilis* 638R AID-1 donor strain, the AID-1 system, and the ATCC 43859 AID-1 recipient. Grey shading indicates homology, red arrows indicate the position of PCR primers used to infer insertion of the AID-1 element at the tRNA-Lys insertion site. **g,** Abundance of *B. ovatus* in samples lacking detected orphan immunity genes (−) and samples in which the indicated orphan immunity genes were assigned to *B. ovatus* (+). Abundances are calculated as in Fig. 1a. (Wilcoxon rank sum test, $*P<0.001$, $n=128$ non-orphan samples and $n=24$ for samples harboring orphan immunity, box plots indicate interquartile range with line at the median and whiskers indicating 1.5 times the IQR).

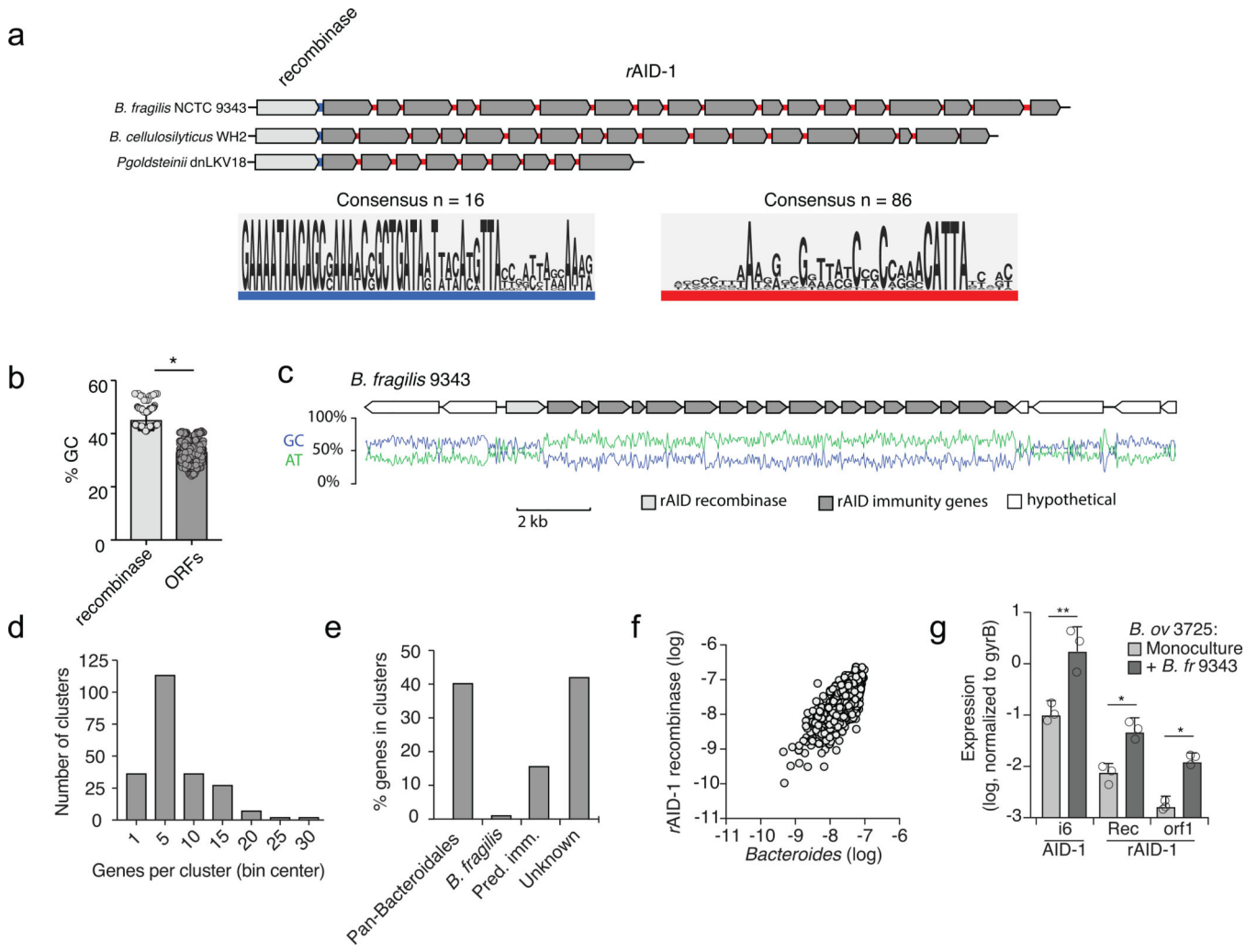

Extended Data Fig. 4 |. The GA2 system of Bacteroidales mediates interbacterial antagonism.
Recovery of *B. dorei* DSM 17855 cells lacking GA2_e14-i14 (BACDOR_RS22955–17020) from two-strain *in vitro* growth competition experiments with the indicated donor strains, n=3 technical replicates representative of three biological replicates, unpaired two-tailed t-test, $^{**}P < 0.01$).

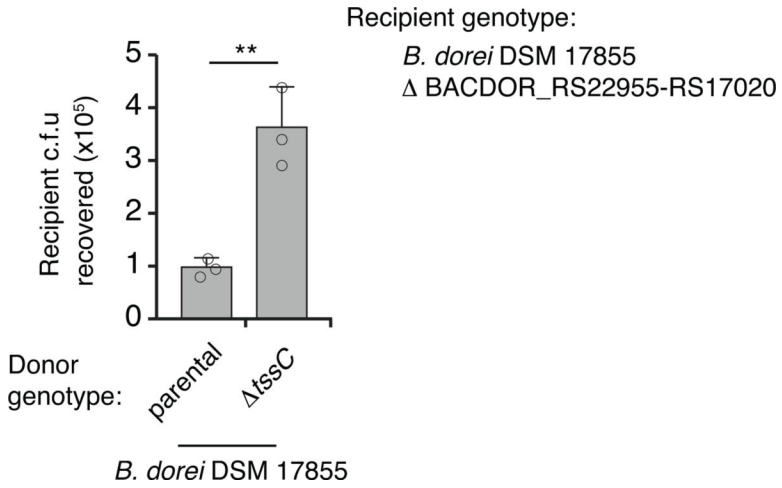

Extended Data Fig. 5 |. *r*AID-1 systems include conserved and repetitive intergenic sequences and bear hallmarks of horizontal gene transfer.

a, Left - Motif enrichment analysis from the intergenic sequences immediately 3' of the recombinase stop codon to the start codon of the first downstream open reading frame within 16 randomly selected rAID-1 gene clusters. This region is highlighted in blue in three representative rAID-1 systems shown above. Right - Motif enrichment analysis from all 86 intergenic sequences between the ORFs of six *r*AID-1 clusters (*B. fragilis* NCTC 9343, *B. cellulosilyticus* WH2, *B. ovatus* 3725, *Paraprevotella clara* YIT 11840, *Parabacteroides goldsteinii* dnLKV18, and *Parabacteroides gordonii* MS-1)[28]. This region is highlighted in red in three representative rAID-1 systems shown above. **b**, Average G+C nucleotide content of *r*AID-1-associated recombinase versus *r*AID-1 predicted ORFs, n=226, unpaired two-tailed t-test, ***P>0.0001. **c,** Schematic depicting the G+C and A+T nucleotide content across a representative *r*AID-1 system from *B. fragilis* 9343. **d,** Frequency distribution of gene number in *r*AID-1 clusters (n=1247 genes in 226 clusters). Bin width is 5 genes. **e,** Composition of genes in *r*AID-1 clusters (n=226 clusters) as determined by profile HMM scans and BLAST analysis against a curated database of Bacteroidales T6SS immunity genes[2,8]. **f,** Comparison of the total abundances of *r*AID-1-associated predicted recombinases and the *Bacteroides* genus in adult microbiome samples derived from the HMP and MetaHIT studies (Supplementary Table 8). Abundance values are calculated as in Fig 1; genus abundance corresponds to the sum of all *Bacteroides* spp. (calculated individually as the average of species-specific marker gene abundances). **g,** Results of qRT-PCR analyses for the indicated *B. ovatus* 3725 genes belonging to AID-1 (i6, M088_1971) or *r*AID-1 clusters (Rec, recombinase, M088_1401; *orf1*, M088_1400) under conditions of growth in mono- or co-culture with *B. fragilis* 9343 for 2 hrs. Data represent mean ± s.d. of n=3 independent biological replicates, Wilcoxon two-tailed sign-rank test, **P < 0.01, *P < 0.05.

Supplementary Material

Refer to Web version on PubMed Central for supplementary material.

Acknowledgements

We thank the UW GNAC for assistance with gnotobiotic experiments. We thank Cynthia Sears, Andy Goodman, Tomomi Kuwahara, and Eric Martens for generously providing *Bacteroides* strains. **Funding:** This work was supported by National Institutes of Health grants AI080609 (to JDM), P30DK089507 (to LRH as pilot study PI), R01DK095869 (to LRH), K99GM129874 (to BDR), R01GM124312 (to EB), and New Innovator Award DP2AT00780201 (to EB), and the Burroughs Wellcome Fund (to JDM). AJV was supported by a postdoctoral fellowship from the Natural Sciences and Engineering Research Council of Canada. BDR was supported by a Simons Foundation-sponsored Life Sciences Research Foundation postdoctoral fellowship. EB is a Faculty Fellow of the Edmond J. Safra Center for Bioinformatics at Tel Aviv University. JDM is an HHMI Investigator.

References

1. Whitney JC et al. A broadly distributed toxin family mediates contact-dependent antagonism between gram-positive bacteria. Elife 6(2017).
2. Zhang D, de Souza RF, Anantharaman V, Iyer LM & Aravind L Polymorphic toxin systems: Comprehensive characterization of trafficking modes, processing, mechanisms of action, immunity and ecology using comparative genomics. Biol Direct 7, 18 (2012). [PubMed: 22731697]
3. Coyne MJ, Roelofs KG & Comstock LE Type VI secretion systems of human gut Bacteroidales segregate into three genetic architectures, two of which are contained on mobile genetic elements. BMC Genomics 17, 58 (2016). [PubMed: 26768901]
4. Russell AB et al. A type VI secretion-related pathway in Bacteroidetes mediates interbacterial antagonism. Cell Host Microbe 16, 227–36 (2014). [PubMed: 25070807]
5. Hood RD et al. A type VI secretion system of Pseudomonas aeruginosa targets a toxin to bacteria. Cell Host Microbe 7, 25–37 (2010). [PubMed: 20114026]
6. Cornforth DM & Foster KR Competition sensing: the social side of bacterial stress responses. Nat Rev Microbiol 11, 285–93 (2013). [PubMed: 23456045]
7. Hille F et al. The Biology of CRISPR-Cas: Backward and Forward. Cell 172, 1239–1259 (2018). [PubMed: 29522745]
8. Verster AJ et al. The Landscape of Type VI Secretion across Human Gut Microbiomes Reveals Its Role in Community Composition. Cell Host Microbe 22, 411–419 e4 (2017). [PubMed: 28910638]
9. Wexler AG et al. Human symbionts inject and neutralize antibacterial toxins to persist in the gut. Proc Natl Acad Sci U S A 113, 3639–44 (2016). [PubMed: 26957597]
10. Hecht AL et al. Strain competition restricts colonization of an enteric pathogen and prevents colitis. EMBO Rep 17, 1281–91 (2016). [PubMed: 27432285]
11. Kirchberger PC, Unterweger D, Provenzano D, Pukatzki S & Boucher Y Sequential displacement of Type VI Secretion System effector genes leads to evolution of diverse immunity gene arrays in Vibrio cholerae. Sci Rep 7, 45133 (2017). [PubMed: 28327641]
12. Steele MI, Kwong WK, Whiteley M & Moran NA Diversification of Type VI Secretion System Toxins Reveals Ancient Antagonism among Bee Gut Microbes. MBio 8(2017).
13. Ting SY et al. Bifunctional Immunity Proteins Protect Bacteria against FtsZ-Targeting ADP-Ribosylating Toxins. Cell (2018).
14. Lloyd-Price J et al. Strains, functions and dynamics in the expanded Human Microbiome Project. Nature 550, 61–66 (2017). [PubMed: 28953883]
15. Qin J et al. A human gut microbial gene catalogue established by metagenomic sequencing. Nature 464, 59–65 (2010). [PubMed: 20203603]
16. Manor O et al. Metagenomic evidence for taxonomic dysbiosis and functional imbalance in the gastrointestinal tracts of children with cystic fibrosis. Sci Rep 6, 22493 (2016). [PubMed: 26940651]
17. Siguier P, Gourbeyre E & Chandler M Bacterial insertion sequences: their genomic impact and diversity. FEMS Microbiol Rev 38, 865–91 (2014). [PubMed: 24499397]
18. Zhao S et al. Adaptive Evolution within Gut Microbiomes of Healthy People. Cell Host Microbe 25, 656–667 e8 (2019). [PubMed: 31028005]

19. Wozniak RA & Waldor MK Integrative and conjugative elements: mosaic mobile genetic elements enabling dynamic lateral gene flow. Nat Rev Microbiol 8, 552–63 (2010). [PubMed: 20601965]
20. Stevens AM, Shoemaker NB & Salyers AA The region of a Bacteroides conjugal chromosomal tetracycline resistance element which is responsible for production of plasmidlike forms from unliked chromosomal DNA might also be involved in transfer of the element. Journal of Bacteriology 172, 4271–4279 (1990). [PubMed: 2165473]
21. Castillo F, Benmohamed A & Szatmari G Xer Site Specific Recombination: Double and Single Recombinase Systems. Front Microbiol 8, 453 (2017). [PubMed: 28373867]
22. Abu-Ali GS et al. Metatranscriptome of human faecal microbial communities in a cohort of adult men. Nature Microbiology 3, 356–366 (2018).
23. Foster KR & Bell T Competition, not cooperation, dominates interactions among culturable microbial species. Curr Biol 22, 1845–50 (2012). [PubMed: 22959348]
24. Poole SJ et al. Identification of functional toxin/immunity genes linked to contact-dependent growth inhibition (CDI) and rearrangement hotspot (Rhs) systems. PLoS Genet 7, e1002217 (2011). [PubMed: 21829394]
25. Drider D, Fimland G, Hechard Y, McMullen LM & Prevost H The continuing story of class IIa bacteriocins. Microbiol Mol Biol Rev 70, 564–82 (2006). [PubMed: 16760314]
26. Coyte KZ, Schluter J & Foster KR The ecology of the microbiome: Networks, competition, and stability. Science 350, 663–6 (2015). [PubMed: 26542567]
27. Li J et al. An integrated catalog of reference genes in the human gut microbiome. Nat Biotechnol 32, 834–41 (2014). [PubMed: 24997786]
28. Bailey TL et al. MEME SUITE: tools for motif discovery and searching. Nucleic Acids Res 37, W202–8 (2009). [PubMed: 19458158]
29. Human Microbiome Project C Structure, function and diversity of the healthy human microbiome. Nature 486, 207–14 (2012). [PubMed: 22699609]
30. Qin J et al. A metagenome-wide association study of gut microbiota in type 2 diabetes. Nature 490, 55–60 (2012). [PubMed: 23023125]
31. Truong DT et al. MetaPhlAn2 for enhanced metagenomic taxonomic profiling. Nat Methods 12, 902–3 (2015). [PubMed: 26418763]
32. Langmead B & Salzberg SL Fast gapped-read alignment with Bowtie 2. Nature Methods 9, 357 (2012). [PubMed: 22388286]
33. Li H et al. The Sequence Alignment/Map format and SAMtools. Bioinformatics 25, 2078–9 (2009). [PubMed: 19505943]
34. Luo R et al. SOAPdenovo2: an empirically improved memory-efficient short-read de novo assembler. Gigascience 1, 18 (2012). [PubMed: 23587118]
35. Besemer J, Lomsadze A & Borodovsky M GeneMarkS: a self-training method for prediction of gene starts in microbial genomes. Implications for finding sequence motifs in regulatory regions. Nucleic Acids Res 29, 2607–18 (2001). [PubMed: 11410670]
36. Bacic MK & Smith CJ Laboratory maintenance and cultivation of bacteroides species. Curr Protoc Microbiol Chapter 13, Unit 13C 1 (2008).
37. Koropatkin NM, Martens EC, Gordon JI & Smith TJ Starch catabolism by a prominent human gut symbiont is directed by the recognition of amylose helices. Structure 16, 1105–15 (2008). [PubMed: 18611383]
38. Degnan PH, Barry NA, Mok KC, Taga ME & Goodman AL Human gut microbes use multiple transporters to distinguish vitamin B(1)(2) analogs and compete in the gut. Cell Host Microbe 15, 47–57 (2014). [PubMed: 24439897]
39. Hoffman LR et al. Escherichia coli dysbiosis correlates with gastrointestinal dysfunction in children with cystic fibrosis. Clin Infect Dis 58, 396–9 (2014). [PubMed: 24178246]
40. Wick RR, Judd LM, Gorrie CL & Holt KE Unicycler: Resolving bacterial genome assemblies from short and long sequencing reads. PLoS computational biology 13, e1005595–e1005595 (2017). [PubMed: 28594827]

41. Martens EC, Chiang HC & Gordon JI Mucosal glycan foraging enhances fitness and transmission of a saccharolytic human gut bacterial symbiont. Cell Host Microbe 4, 447–57 (2008). [PubMed: 18996345]

42. Garcia-Bayona L & Comstock LE Bacterial antagonism in host-associated microbial communities. Science 361(2018).

43. Lim B, Zimmermann M, Barry NA & Goodman AL Engineered Regulatory Systems Modulate Gene Expression of Human Commensals in the Gut. Cell 169, 547–558.e15 (2017). [PubMed: 28431252]

44. Paik J et al. Potential for using a hermetically-sealed, positive-pressured isocage system for studies involving germ-free mice outside a flexible-film isolator. Gut Microbes 6, 255–65 (2015). [PubMed: 26177210]

45. Silverman JM et al. Haemolysin coregulated protein is an exported receptor and chaperone of type VI secretion substrates. Mol Cell 51, 584–93 (2013). [PubMed: 23954347]

46. Cardona ST & Valvano MA An expression vector containing a rhamnose-inducible promoter provides tightly regulated gene expression in Burkholderia cenocepacia. Plasmid 54, 219–28 (2005). [PubMed: 15925406]

47. Bookout AL, Cummins CL, Mangelsdorf DJ, Pesola JM & Kramer MF High-throughput real-time quantitative reverse transcription PCR. Curr Protoc Mol Biol Chapter 15, Unit 15 8 (2006).

48. Caro-Quintero A & Ochman H Assessing the Unseen Bacterial Diversity in Microbial Communities. Genome Biol Evol 7, 3416–25 (2015). [PubMed: 26615218]

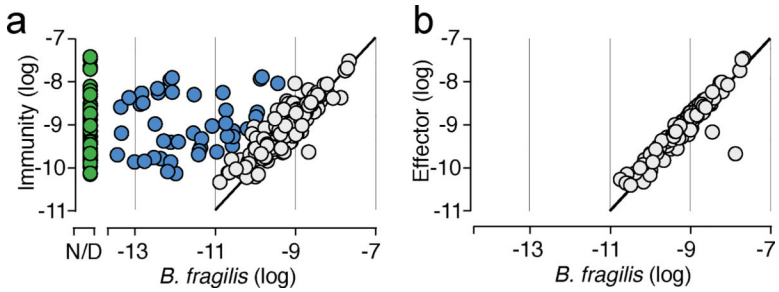

Fig. 1 |. T6SS orphan immunity genes are found in human gut microbiomes.

Abundance comparison of *B. fragilis*-specific T6SS immunity genes **a** or effector genes **b** with *B. fragilis* marker genes in adult microbiome samples derived from the HMP and MetaHIT studies (Supplementary Table 1). Abundance values denote the number of reads mapped to the gene, normalized by gene length and total number of reads in the sample. Abundances are calculated as the average abundance of all immunity, effector, or *B. fragilis* species-specific marker genes. Samples with undetectable *B. fragilis* (green) and samples in which immunity gene abundance exceeds that of *Bacteroides* by over 10-fold (blue) are highlighted.

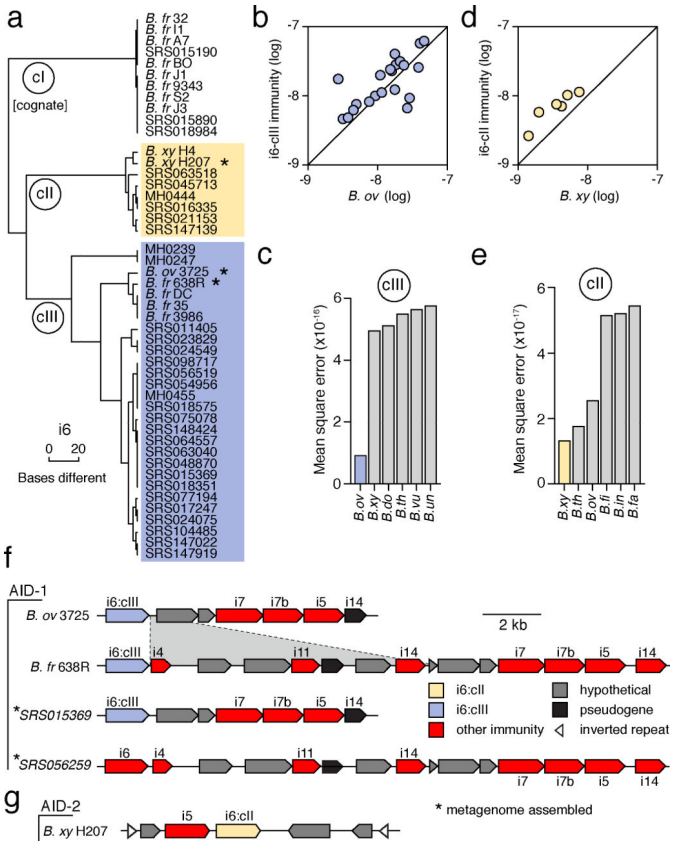

Fig. 2 |. T6SS orphan immunity gene clusters are encoded by multiple species in the human gut microbiome.

a, Dendrogram depicting hierarchical clustering of orphan immunity gene i6 sequences extracted from genomes (n=15) and metagenomes (n=32) derived from the indicated HMP (SRS) or MetaHIT (MH) samples. Sequence clades discussed in the text are denoted (cI-III). Asterisks indicate strains diagrammed in panels **f** and **g**. **b-d** Abundance comparison of genes from the indicated immunity clades (colors as in **a**) with *B. ovatus* **b** or *B. xylanisolvens* **d** marker genes in adult microbiome samples (Supplementary Table 1). **c, e,** Linear model error values for the six species best fitting i6:cIII **c** and i6:cII **e** gene abundances calculated as in Fig. 1. **f, g**, Representative AID-1 **f** and AID-2 **g** gene clusters containing homologs of the indicated *B. fragilis* T6S immunity genes. The i6 gene of SRS056259 did not meet our sequence depth coverage requirements for inclusion in i6:cIII. The *B. xylanisolvens* strain in **g** was sequenced as a part of this study (BioProject PRJNA484981). A region of difference between *B. ovatus* 3725 and *B. fragilis* 638R clusters is highlighted. All strain abbreviations defined in Supplementary Table 3.

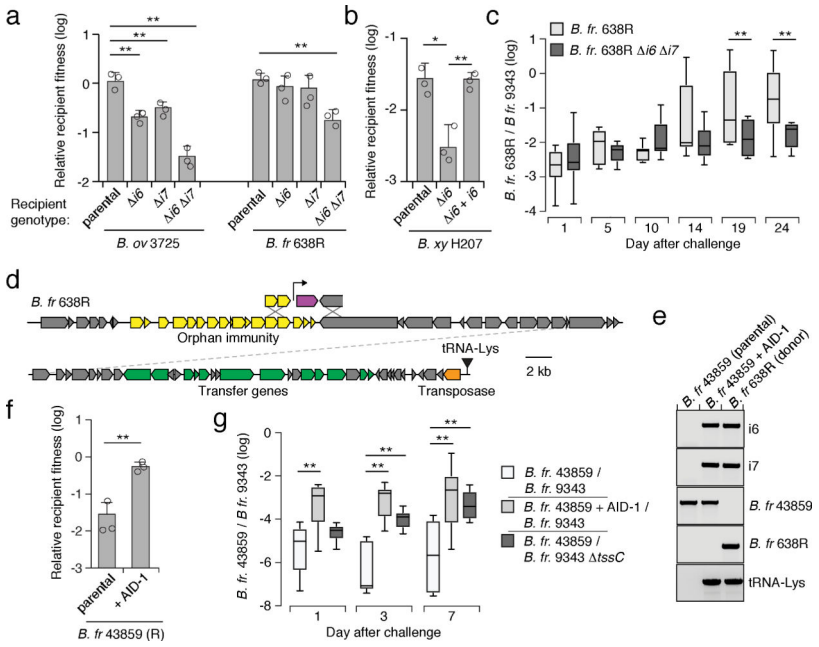

Fig. 3 |. Orphan immunity genes are mobile and protect against T6S-delivered toxins.

a, b, Outcomes of growth competition assays between the indicated AID-1 **a** or AID-2 **b** harboring strains versus *B. fragilis* 9343. Relative recipient fitness was determined by calculating the ratio of final to initial colony forming units (c.f.u.) and normalizing to corresponding experiments with T6S-inactive *B. fragilis* 9343 (Δ*tssC*). Data represent mean ± s.d. of n=3 technical replicates indicative of at least three biological replicates,* $P < 0.05$, ** $P < 0.01$, (unpaired two-tailed t-test). **c**, Outcome of pairwise competition between the indicated *B. fragilis* strains in germ-free mice. Mice were colonized with *B. fragilis* 9343 for one week and challenged with 638R (n=8 mice per group for each of two independent experiments). Boxplots represent the interquartile range with indicated means for each group, whiskers represent the minimum and maximum values, ** $P < 0.01$ (Mann-Whitney U test for each time point). **d**, Schematic depicting a *B. fragilis* 638R ICE harboring the AID-1 cluster depicted in Fig. 2f. **e**, PCR analysis of an AID-1 transfer experiment. Schematic with primer locations provided in Extended Data Fig. 3f. Transfer data are representative of two independent biological replicates. **f**, Outcomes of growth competition assays between *B. fragilis* 43859 or a derivative AID-1 ICE recipient and *B. fragilis* 9343. Data presentation and statistics as in **a,b. g**, Results of pairwise competition between the indicated *B. fragilis* strains in germ-free mice (n=6 mice from two independent experiments). Statistics, and data presentation performed as in **c**.

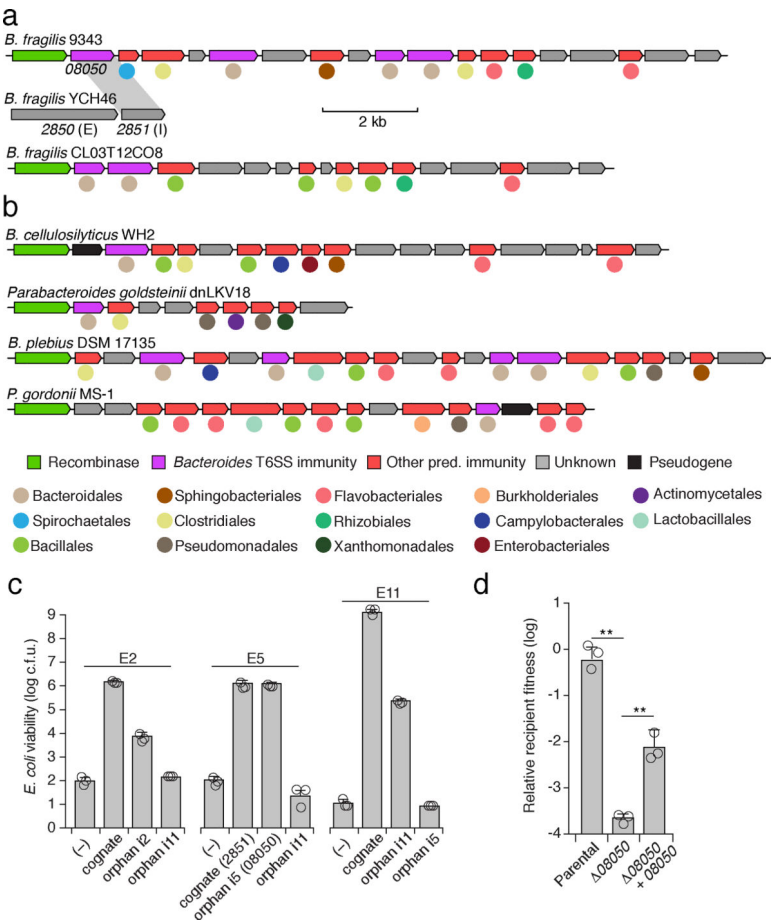

Fig. 4 |. *r*AID systems encode toxin-neutralizing immunity genes and are prevalent in human gut microbiomes.

a, b, *r*AID-1 clusters from the indicated *B. fragilis* **a**, or Bacteroidales **b**, species. *r*AID-1 genes were assigned to functional immunity classes (indicated by gene coloring) via profile HMM scans and BLAST against a curated database of Bacteroidales T6SS immunity genes[2,8]. Colored circles indicate taxonomic association of the top non-*r*AID-1 homolog. Homology (70% a.a. identity) between gene 08050 of the *B. fragilis* 9343 *r*AID-1 cluster and a T6S cognate immunity gene from *B. fragilis* YCH46 (2851) is indicated. **c**, Viable *E. coli* cells recovered from cultures expressing indicated proteins (refer to Supplementary Table 10 for locus tags). Data indicate n=3 technical replicates representative of 3 independent biological replicates, bars indicate mean ± s.d. **d**, Outcomes of growth competition assays between the indicated *Bacteroides* strains (n=3 biologically independent samples). The relevant *r*AID-1 gene of *B. fragilis* 9343 and its corresponding effector within *B. fragilis* YCH46 are depicted in **a**. Statistics were performed using unpaired two-tailed *t*-tests, ** $P>0.01$, bars indicate mean ± s.d.